34th Annual International Conference of the IEEE EMBS
San Diego, California USA, 28 August - 1 September, 2012

Automatic image-based retrospective gating of interventional cardiac X-ray images

Maria Panayiotou, Andrew P. King, YingLiang Ma, C. Aldo Rinaldi, J. Gill, Michael Cooklin, Mark O'Neill and Kawal S. Rhode

Abstract— **Gating of X-ray fluoroscopy images is required for catheter reconstruction for registration of pre-procedural images with fluoroscopy for guidance and biophysical modelling. We propose a novel and clinically useful retrospective method for automatic image-based cardiac and respiratory motion gating. The technique is based on tracking and statistical analysis of the shape of the coronary sinus catheter. We applied our method on five mono-plane imaging sequences comprising a total of 322 frames from five different patients undergoing radiofrequency ablation for the treatment of atrial fibrillation. We established systole, end-inspiration and end-expiration gating with success rates of 100%, 89.47% and 81.25% respectively.**

I. INTRODUCTION

Minimally-invasive catheter procedures are routinely used to treat heart disease. Electrophysiology (EP) procedures are an example and are used to treat patients with rhythm disorders. These procedures are carried out under X-ray fluoroscopic image guidance. X-ray fluoroscopy has several drawbacks, such as poor soft tissue contrast and the delivery of radiation dose. In order to address these issues, image fusion can be used where pre-procedural three-dimensional (3D) images can be combined with the 2D X-ray images for roadmapping. The 2D-3D registration can be achieved using specialised hybrid imaging systems [1]. However, achieving the registration in a conventional mono-plane catheter laboratory is challenging. A promising solution is the use of catheters to constrain the registration [2]. A recent implementation of this approach uses 3D catheter reconstructions from sequential biplane X-ray images [3]. This technique requires both cardiac and respiratory phase matching of the biplane images. In [3], this was achieved manually, but an automatic technique would significantly speed up the clinical workflow. A similar requirement for automatic frame matching exists when catheter positional information needs to be measured with reference to a registered anatomical model. This can be useful for recording the position of electrical measurements, pacing locations and ablation treatments [4, 5].

Cardiac gating can be achieved by synchronously recording the electrocardiogram (ECG) with the X-ray images. However, this is not a standard feature on commercial X-ray systems and, when present, there may be unknown latency between the acquisition of the ECG and X-ray data. Respiratory gating can be achieved using the breath-hold technique that is commonly used during magnetic resonance imaging [6, 7]. However, this is not practical in the catheter laboratory where patients can be heavily sedated. Respiratory phase determination by diaphragm tracking was demonstrated in [8]. This is an accurate and robust approach but the diaphragm is not always visible in cardiac X-ray images due to collimation to reduce radiation dose. A more promising approach is to track the EP catheters [9, 10, 11]. The disadvantage of this technique is that uncoupling the cardiac from the respiratory motion can be challenging. Another promising approach was presented in [12]. This technique estimates the motion between successive frames using the phase correlation algorithm and was tested using X-ray coronary angiography images. However, the performance of this approach for EP images containing high-contrast catheters is not known.

We propose a novel approach for cardiac and respiratory phase determination for cardiac EP X-ray images based on principal component analysis (PCA) of tracked catheter electrodes. The algorithm is validated using X-ray images taken during radiofrequency ablation procedures (RFA) for patients being treated for atrial fibrillation (AF). Manual identification of systole was used as the gold standard for cardiac gating and diaphragm or heart border tracking [13] was used as the gold standard for respiratory gating.

II. METHODS

The proposed method comprises three main steps. Firstly, the technique described in [11] is used to track the electrodes of the coronary sinus (CS) catheter throughout the X-ray sequence. This catheter is routinely used during EP procedures and provides reference information to the cardiologist throughout the procedure. Secondly, PCA is applied to the coordinates of the tracked electrodes. Thirdly, the results of the PCA are processed to provide automatic cardiac and respiratory gating. These individual steps are described below.

A. *Data acquisition*

All patient procedures were carried out using a mono-plane flat-panel cardiac X-ray system (Philips Allura Xper FD10, Philips Healthcare, Best, The Netherlands).

B. *Coronary sinus catheter detection*

The CS catheter is composed of 10 electrodes, distributed in pairs along the catheter (see figure 1). The CS catheter tracking technique [11] uses a fast multi-scale blob detection method to detect all electrode-like objects in an X-ray image and a cost function to discriminate the CS catheter from other catheters. Manual tracking was performed in cases

Maria Panayiotou, Andrew P. King, YingLiang Ma and Kawal S. Rhode are with the Division of Imaging Sciences & Biomedical Engineering, King's College London, SE1 7EH, UK. (phone: +44(0)7517477702; e-mail: mariapanayiotou@kcl.ac.uk).

C. Aldo Rinaldi, J. Gill, Michael Cooklin and Mark O'Neill are with the Department of Cardiology, Guy's & St. Thomas' Hospitals NHS Foundation Trust, London, SE1 7EH, UK.

where the technique failed to detect electrodes. After application of the tracking algorithm, the x and y positions of each of the 10 electrodes were concatenated into a single column vector. Hence, the data generated by the tracking process consisted of:

$$\mathbf{s}_i = (z_{i,1,x}, z_{i,1,y}, .. z_{i,10,x}, z_{i,10,y})^T, 1 \le i \le N \quad (1)$$

where $z_{i,e,x}$ and $z_{i,e,y}$ represent the x and y coordinates, in pixels, of the eth electrode in the frame and N is the number of frames.

C. Principal component analysis (PCA)

PCA transforms a multivariate dataset of possibly correlated variables into a new dataset of a smaller number of uncorrelated variables called principal components (PCs), without any loss of information. We first compute the mean vector:

$$\bar{\mathbf{s}} = \frac{1}{N}\sum_{i=1}^{N}\mathbf{s}_i \quad (2)$$

and the covariance matrix:

$$\mathbf{S} = \frac{1}{N}\sum_{i=1}^{N}(\mathbf{s}_i - \bar{\mathbf{s}})(\mathbf{s}_i - \bar{\mathbf{s}})^T \quad (3)$$

according to the standard PCA technique. The eigenvectors $\mathbf{v}_m$, $1 \le m \le M$ of $\mathbf{S}$ represent the PCs and the corresponding eigenvalues d_m, $1 \le m \le M$ represent the variance of the data along the direction of the eigenvectors. For our application M=20 since the $\mathbf{s}_i$ are of length 20, although at most N-1 of these will have non-zero eigenvalues. Next, to estimate the contribution of each of the PCs to the variation in the electrode positions, we compute the scalar projection of the original data onto each of the (unit) PC vectors:

$$P_{m,i} = \mathbf{v}_m \bullet (\mathbf{s}_i - \bar{\mathbf{s}}), 1 \le m \le M, 1 \le i \le N \quad (4)$$

The hypothesis is that the PCA will extract the cardiac and respiratory modes and that $P_{m,i}$ will therefore represent cardiac/respiratory signals that can be used for gating. It was found by visual inspection that the variation of 1st PC was dominated by cardiac motion and that the variation of the 2nd PC was dominated by respiratory motion for all datasets that we analysed.

D. Cardiac gating

The 1st PC is used to detect systolic (sys) frames of the image sequences which are represented by the peaks of the variation of the 1st PC with frame number;

$$\Omega_{sys} = \{i \mid P_{1,i-1} < P_{1,i} > P_{1,i+1}\} \quad (5)$$

where Ω_{sys} is the set of all frame numbers that are identified as systole.

E. Respiratory gating

The 2nd PC relates to the respiratory motion. However, some cardiac motion remains. To eliminate the effect of the cardiac motion we gate the variation of the 2nd PC using the peaks of the variation of the 1st PC. Hence, end-inspiration (EI) and end-expiration (EX) are represented by:

$$\Omega_{sys,EI} = \{i \mid P_{2,j} < P_{2,i} > P_{2,k}, i, j, k \in \Omega_{sys}, j < i < k\} \quad (6)$$

and

$$\Omega_{sys,EX} = \{i \mid P_{2,j} > P_{2,i} < P_{2,k}, i, j, k \in \Omega_{sys}, j < i < k\} \quad (7)$$

respectively, where j, i and k are temporally consecutive systolic frames.

III. RESULTS

We validated our method on 5 clinical fluoroscopy sequences from 5 patients who underwent RFA procedures for the treatment of AF. For each patient, X-ray imaging was performed at 3 frames per second. A total of 322 frames were processed. The percentages of variation in PCs 1 and 2 for each patients were calculated to be 95.6%, 87.7%, 89.6%, 93.2%, 78.9% for the 1st PC and 3.2%, 11.2%, 8.4%, 5.52%, 20.5% for the 2nd PC, respectively. Because our technique is intended for retrospective analysis, we did not separate training and test data. Rather, all frames were used for both training and testing the model.

A. Qualitative Validation

In order to qualitatively validate our cardiac gating method, manual gating of the cardiac cycle at systole was performed by an experienced observer, by visually detecting the onset of contraction of the left ventricle from the fluoroscopic left heart border shadow. The systolic frame number was recorded and compared against the corresponding systolic frame number from the automatic detection. We chose systole as opposed to diastole for validation since the manual ground truth is more reliable for systole where rapid motion can be used as the visual clue. Plots of the data with respect to the 1st PC for the first 30 frames for two example X-ray sequences are illustrated in figures 1(b) and 2(b). The plotted vertical black lines correspond to the gold standard systolic frames. The first image of the processed X-ray sequences is shown in figures 1(a) and 2(a).

We validated the respiratory gating using either diaphragm or heart border tracking as described in [13] for the ground truth. The choice of ground truth was determined by which structure was visible in the X-ray images. The respiratory signal obtained from diaphragm/heart border tracking was cardiac gated using the manually identified systolic frames. The peaks/troughs obtained using the tracking method were compared to the peaks/troughs obtained using the PCA-based method. The results are shown in Figure 3 for two patient cases. Our PCA-based technique is shown in blue. The diaphragm tracking (gold standard) is shown in green.

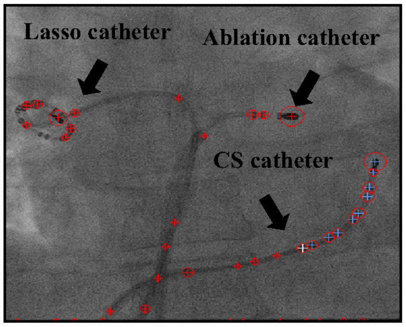

(a)

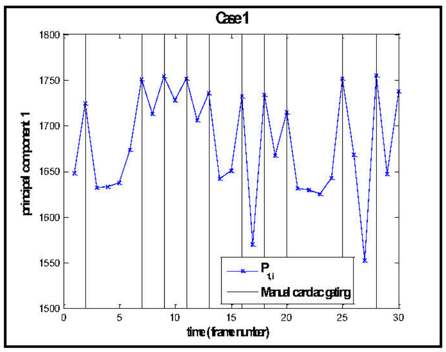

(b)

Figure 1. (a) Case 1: Example X-ray image showing the different types of EP catheters during the ablation stage of a procedure to treat AF. The CS catheter electrodes have been differentially detected by the algorithm in [11]; (b) Graphical representation of the variation of the 1st PC with X-ray frame number. The black lines are the gold standard identification of systole.

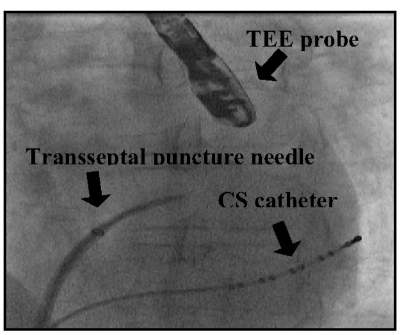

(a)

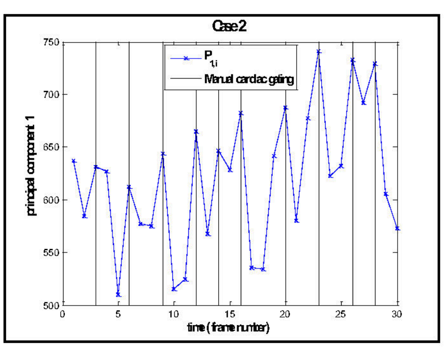

(b)

Figure 2. (a) Case 2: Example X-ray image during the transseptal puncture stage of a procedure to treat AF; (b) Graphical representation of the variation of the 1st PC with X-ray frame number.

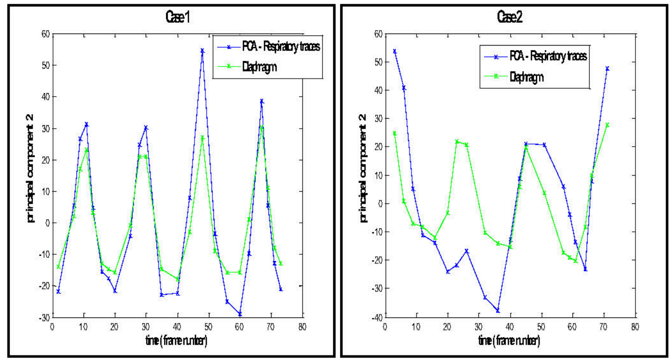

(a) (b)

Figure 3. The respiratory traces obtained after applying the PCA-based method are illustrated for Case1 (a) and Case2 (b) in blue. The diaphragm tracking (gold standard) is also shown for (a) case 1 and (b) case 2.

B. *Comparative quantitative validation*

It was important to investigate whether the new PCA-based technique was superior to simply using the Cartesian coordinates of the electrode positions alone. Therefore, as a comparative technique, the tracking data for the proximal and distal electrodes of the CS catheter were employed using the same gating technique. Specifically, for the proximal electrode the x coordinate, $z_{i,1,x}$ was used in place of $P_{1,i}$ and the y-coordinate, $z_{i,1,y}$ was used in place of $P_{2,i}$. Similarly, for the distal electrode the x coordinate, $z_{i,10,x}$ was used in place of $P_{1,i}$ and the y-coordinate, $z_{i,10,y}$ was used in place of $P_{2,i}$.

For both cardiac and respiratory gating, the frame difference was computed between the PCA-based methods and the gold standard methods. This was also done for the proximal/distal electrode tracking technique. The results can be seen in figure 4. Our proposed PCA-based technique outperforms both of the alternative electrode position based techniques for all three gating tasks.

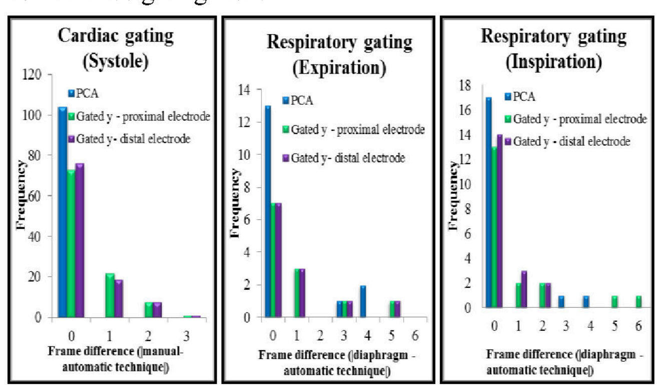

(a) (b) (c)

Figure 4. (a) Cardiac gating performance (b) EX respiratory gating performance (c) EI respiratory gating performance

Table I summarises the number of false positives and false negatives (i.e. extra/fewer detected peaks/troughs) over all processed sequences for all techniques. Table II displays the percentage success rates and Table III indicates the results of statistically analyzing the three techniques. A 2-tailed paired t-test was conducted under the null hypothesis that there was no difference in the techniques. The t-test was done on the absolute frame differences of each of the techniques and was conducted for systole, end-inspiration and end-expiration, only including peaks/troughs that were detected by all three methods. In all cases our proposed PCA-based technique was found to have significantly lower errors than the alternative techniques ($p < 0.05$). The results confirm the accuracy and robustness of the PCA-based gating method.

TABLE I. MISSDETECTION OF PEAKS/TROUGHS

Overall extra; fewer peaks or troughs for 5 clinical sequences			
Automatic technique	***Systole gating***	***EX gating***	***EI gating***
PCA	3; 0	0; 0	0; 0
Gated y – proximal el	7; 0	5; 3	6; 0
Gated y – distal el	7; 0	5; 3	6; 0

TABLE II. % SUCCESS RATE

Success Rate (%)			
Automatic technique	***Systole gating***	***EX gating***	***EI gating***
PCA	100	81.25	89.47
Gated y – proximal el	70.19	43.75	68.42
Gated y – distal el	73.08	43.75	73.68

TABLE III. STATISTICAL ANALYSIS FOR THE AUTOMATIC TECHNIQUES

Mean frame difference; Standard deviation			
Automatic technique	***Systole gating***	***EX gating***	***EI gating***
PCA	0; 0	0.41; 1.08	0.21; 0.80
Gated y – proximal el	0.28; 0.58	1.38; 2.06	0.82; 1.59
Gated y – distal el	0.24; 0.55	1.47; 1.99	0.55; 1.33

IV. DISCUSSION AND CONCLUSION

We have presented an accurate and robust retrospective PCA-based method for image-based automatic cardiac and respiratory motion gating based on catheter shape. This method is able to detect cardiac and respiratory phases from X-ray fluoroscopy images. We have applied our technique on five clinical fluoroscopy sequences and computed the success rates for systolic cardiac gating, EI and EX respiratory gating which were 100%, 89.47% and 81.25%, respectively. The PCA-based method is fully automatic, requiring no user interaction and operates within a few seconds per image sequence. The method has potential application in more types of cardiac catheterization procedures, rather than only RFA procedures. The method will be particularly useful for catheter reconstruction for registration and overlay of pre-procedural images with X-ray fluoroscopy for guidance and biophysical modelling. In future work we plan to investigate non-linear approaches as an alternative to PCA in our statistical model.

ACKNOWLEDGMENT

This work is funded by EPSRC programme grant EP/H046410/1.

REFERENCES

[1] K.S. Rhode, D.L.G. Hill, P.J. Edwards, J. Hipwell, , D. Rueckert, , G. Sanchez-Ortiz, , S. Hegde, V. Rahunathan and R. Razavi, “Registration and tracking to integrate X-ray and MR images in an XMR facility,” IEEE Transactions on Medical Imaging, 24 (11), 2003, pp. 810-815.

[2] J. Sra, G. Narayan, D. Krum, A. Malloy, R. Cooley, A. Bhatia, A. Dhala, Z. Blanck, V. Nangia and M. Akhtar, “Computed tomography-fluoroscopy image integration-guided catheter ablation of atrial fibrillation,” Journal of Cardiovascular Electrophysiology, 18 (4), 2007, pp. 409-14.

[3] M.V. Truong, T. Gordon, R. Razavi, G.P. Penney and K.S. Rhode, “Analysis of Catheter-Based Registration with Vessel-Radius Weighting of 3D CT Data to 2D X-ray for Cardiac Catheterisation Procedures in a Phantom Study,” MICCAI Workshop STACOM 2011.

[4] K.S. Rhode, M. Sermesant, D. Brogan, S. Hegde, J. Hipwell, P. Lambiase, E. Rosenthal, , C. Bucknall, S.A. Qureshi, J.S. Gill, R. Razavi and D.L.G. Hill, “A system for real-time XMR guided cardiovascular intervention,” IEEE Trans. Med. Imag. 24 (11), 2005, pp.1428-1440.

[5] M. Sermesant, R. Chabiniok, P. Chinchapatnam, T. Mansi, F. Billet, P. Moireau, JM. Peyrat, K. Wong, J. Relan, K. Rhode, M. Ginks, P. Lambiase, H. Delingette, M. Sorine, CA. Rinaldi, D. Chapelle, R. Razavi and N. Ayache, “Patient-specific electromechanical models of the heart for the prediction of pacing acute effects in CRT,” a preliminary clinical validation, Med Image Anal, Jan 2012, pp. 201-15.

[6] M.R. Paling and J.R. Brookeman, “Respiration artifacts in MR imaging: reduction by breath holding,” J. Comput. Assist. Tomogr. 10(6), 1986, pp. 1080–1082.

[7] G.S. Mageras and E.Yorke, “Deep inspiration breath hold and respiratory gating strategies for reducing organ motion in radiation treatment,” Semin. Radiat. Oncol. 14(1), 2004, pp. 65–75.

[8] G. Shechter, C. Ozturk, JR. Resar and ER. McVeigh, “Respiratory motion of the heart from free breathing coronary angiograms,” IEEE Trans Med Imaging. Aug 2004, pp. 1046-56.

[9] A. Brost, R. Liao, J. Hornegger and N. Strobel, “3-D Respiratory Motion Compensation during EP Procedures by Image-Based 3-D Lasso Catheter Model Generation and Tracking,” in 12th International Conference on Medical Image Computing and Computer-Assisted Intervention (MICCAI) 2009, London, UK, ser. Lecture Notes in Computer Science, G.-Z. Yang, D. Hawkes, D. Rueckert, J. Noble, and C. Taylor, Eds. Springer Berlin / Heidelberg, 2009, vol. 5761, pp. 394–401.

[10] A. Brost, R. Liao, J. Hornegger and N. Strobel, “Model-Based Registration for Motion Compensation during EP Ablation Procedures,” in Biomedical Image Registration, ser. Lecture Notes in Computer Science, B. Fischer, B. Dawant, and C. Lorenz, Eds. Springer Berlin/ Heidelberg, 2010, vol. 6204, pp. 234–245.

[11] Y. Ma, A.P. King, N. Gogin, C.A. Rinaldi, J. Gill, R. Razavi, K.S. Rhode, “Real-time respiratory motion correction for cardiac electrophysiology procedures using image-based coronary sinus catheter tracking,” In: Jiang, T., Navab, N., Pluim, J.P.W., Viergever, M.A. (eds.) MICCAI 2010. LNCS, vol. 6361, pp. 391–399. Springer, Heidelberg (2010).

[12] H. Sundar, A. Khamene, L. Yatziv, W. Wein, C. Xu, “Automatic image-based cardiac and respiratory cycle synchronization and gating of image sequences,” In: Yang, G.-Z., et al. (eds.) MICCAI 2009, Part I. LNCS, vol. 5761, pp. 381–388. Springer, Heidelberg (2009).

[13] Y. Ma, AP. King, N. Gogin, G. Gijsbers, CA. Rinaldi, J. Gill, R. Razavi, KS. Rhode, “Clinical evaluation of respiratory motion compensation for anatomical roadmap guided cardiac electrophysiology procedures,” IEEE Trans Biomed Eng. 2012 Jan, pp. 122-31.